Inhibitory Mechanism of *FAT4* Gene Expression in Response to Actin Dynamics during Src-Induced Carcinogenesis

Takao Ito¤, Hiroaki Taniguchi, Kousuke Fukagai, Shota Okamuro, Akira Kobayashi*

Laboratory for Genetic Code, Graduate School of Life and Medical Sciences, Doshisha University, Kyotanabe, Kyoto, Japan

¤ Current address: Laboratory of Genetics, Graduate School of Biostudies, Kyoto University, Yoshida-Konoe-cho, Kyoto, Japan

* akobayas@mail.doshisha.ac.jp

Abstract

Oncogenic transformation is characterized by morphological changes resulting from alterations in actin dynamics and adhesive activities. Emerging evidence suggests that the protocadherin FAT4 acts as a tumor suppressor in humans, and reduced *FAT4* gene expression has been reported in breast and lung cancers and melanoma. However, the mechanism controlling *FAT4* gene expression is poorly understood. In this study, we show that transient activation of the Src oncoprotein represses *FAT4* mRNA expression through actin depolymerization in the immortalized normal human mammary epithelial cell line MCF-10A. Src activation causes actin depolymerization via the MEK/Erk/Cofilin cascade. The MEK inhibitor U0126 blocks the inhibitory effect of Src on *FAT4* mRNA expression and Src-induced actin depolymerization. To determine whether actin dynamics act on the regulation of *FAT4* mRNA expression, we treated MCF-10A cells with the ROCK inhibitor Y-27632. Y-27632 treatment decreased *FAT4* mRNA expression. This suppressive effect was blocked by siRNA-mediated knockdown of Cofilin1. Furthermore, simultaneous administration of Latrunculin A (an actin depolymerizing agent), Y-27632, and Cofilin1 siRNA to the cells resulted in a marked reduction of *FAT4* mRNA expression. Intriguingly, we also found that *FAT4* mRNA expression was reduced under both low cell density and low stiffness conditions, which suggests that mechanotransduction affects *FAT4* mRNA expression. Additionally, we show that siRNA-mediated FAT4 knockdown induced the activity of the Hippo effector YAP/TAZ in MCF-10A cells. Taken together, our results reveal a novel inhibitory mechanism of *FAT4* gene expression through actin depolymerization during Src-induced carcinogenesis in human breast cells.

Introduction

Oncogenic cell transformation results from the summation of changes in cell growth, cell viability, cell motility and cell morphology. The v-Src oncogene, a product of the Rous sarcoma

virus, is the constitutively active form of c-Src. Src has the ability to regulate various signal transduction pathways, including the Ras/MEK/Erk, PI3K/Akt, STAT3, and Rho/ROCK pathways [1–4]. More specifically, Src has been reported to induce alterations in cell morphology through actin dynamics and to depolymerize the actin cytoskeleton via the MEK/Erk/Cofilin cascade [5]. Additionally, members of the cadherin superfamily have been implicated in Src-induced tumor transformation. Src downregulates E-cadherin expression and triggers morphological changes in multiple cancers [6–8]. These findings suggest the importance of both actin dynamics and the loss of cadherin-mediated cell-cell adhesion in Src-induced tumorigenesis.

FAT4, a protocadherin, is the human ortholog of *Drosophila* Fat [9,10]. Recent studies indicate that *Drosophila* Fat suppresses tumorigenesis through activation of the Hippo pathway. In support of this finding, PrognoScan, a new microarray database [11], and other recent studies [12–14] have demonstrated that human *FAT4* gene expression is repressed in breast and lung cancers and in melanoma, which suggests that reduced *FAT4* gene expression can trigger carcinogenesis. However, the molecular mechanisms underlying the down-regulation of *FAT4* gene expression in human cancers remain unknown.

The Hippo pathway is involved in tumor suppressor signaling and regulates organ size, cell proliferation, apoptosis and stemness [9,10,15,16]. In mammals, the core components of the Hippo pathway are primarily composed of Mst1/2 and Lats1/2, which inactivate the Hippo effector Yap/Taz via phosphorylation [17–22]. Yap/Taz acts as a transcriptional co-activator by binding the transcription factors Tead1–4 to induce the expression of genes such as the connective tissue growth factor CTGF [18,23,24]. Fat4 has been shown to repress Yap activity and thereby negatively regulates neural progenitor cell proliferation during mammalian neurogenesis [25,26]. Thus, the FAT4-Hippo axis is believed to be functionally conserved in humans; however, the functional significance and the molecular mechanisms that confer this axis are poorly understood.

Here, we show that transient Src activation represses *FAT4* mRNA expression and leads to tumor transformation in MCF-10A cells, which are immortalized normal human mammary epithelial cells. We further demonstrate that the inhibitory effect of Src on *FAT4* mRNA expression depends on actin depolymerization that is induced by the MEK/Erk/Cofilin cascade. Finally, we demonstrate that FAT4 represses YAP/TAZ activity in MCF-10A cells.

Results

FAT4 gene expression is repressed during human breast cell transformation by the Src oncogene

To analyze the mechanisms that repress *FAT4* gene expression in human breast cancer, we generated a model of carcinogenesis using MCF-10A cells, an immortalized normal human mammary epithelial cell line [27–31]. In brief, we used retroviruses to create MCF-10A cells that stably express the Src kinase oncoprotein (v-Src) fused to the ligand binding domain of the estrogen receptor (ER). In MCF-10A v-Src:ER cells, the addition of 4-Hydroxytamoxifen (TAM) induces Src activation and their subsequent cell transformation. TAM treatment resulted in morphological transformation (Fig. 1A), enhanced cell proliferation (Fig. 1B), and promoted anchorage-independent growth (Fig. 1C). In this model, we found that *FAT4* mRNA expression was repressed by Src activation in MCF-10A cells (Fig. 1D). On the other hand, *TWIST1* mRNA expression was not altered under similar experimental conditions (S1 Fig.). This points to the specificity of the inhibitory effect of Src on *FAT4* mRNA expression. Thus, these results indicate that Src induces tumorigenesis and suppresses *FAT4* mRNA expression in MCF-10A cells.
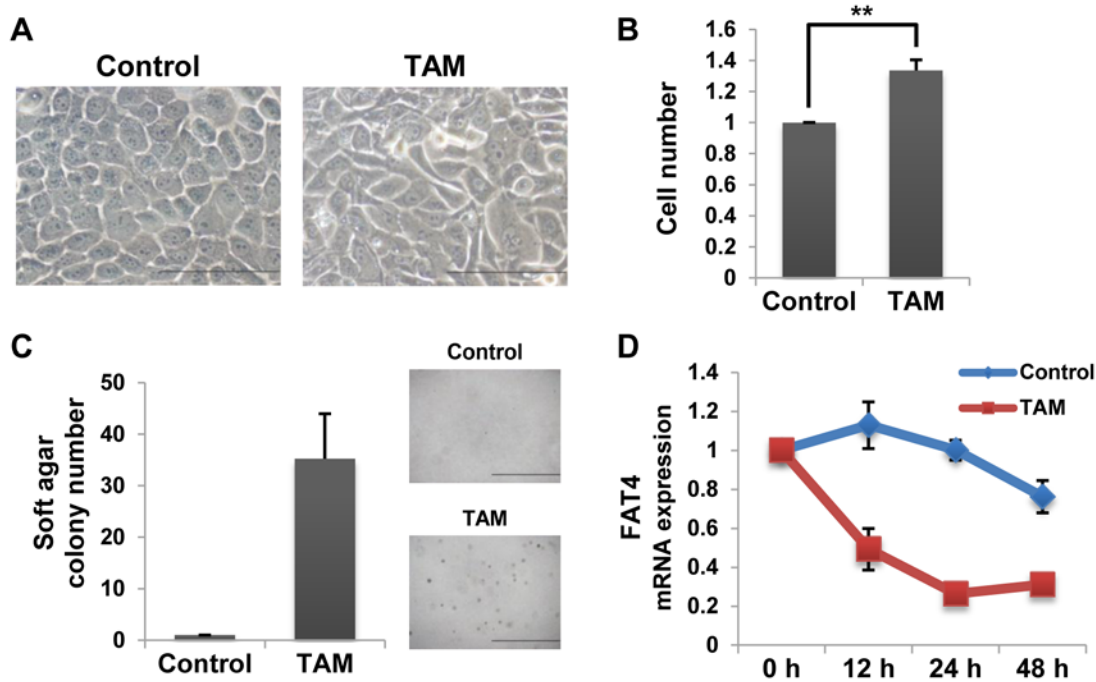
Fig 1. Transient activation of Src depresses *FAT4* gene expression and induces tumor transformation in MCF-10A cells. A. Images show morphological changes of MCF-10A v-Src:ER cells treated with 1 µM TAM for 36 h. Black bars, 100 µm. **B**. WST-1 Assay in TAM-treated cells (48 h) (mean ± SD, n = 3, ** indicates $P < 0.01$). **C**. Soft Agar Colony Formation Assay in TAM-treated cells (72 h) (mean ± SD, n = 4). Images show cell colonies. Black bars, 1 mm. **D**. RT-qPCR analysis of *FAT4* mRNA expression levels in TAM-treated cells for the indicated times (mean ± SD, n = 3).

doi:10.1371/journal.pone.0118336.g001

Src activation induces both *FAT4* gene repression and Cofilin-mediated actin depolymerization through the MEK/Erk pathway

Src has been shown to elicit Cofilin-mediated disruption of the actin cytoskeleton through the MEK/Erk pathway [5]. The function of Cofilin is activated via its dephosphorylation [32]. Thus, we examined whether Src can disrupt the actin cytoskeleton through dephosphorylation of Cofilin in MCF-10A v-Src:ER cells. Indeed, phalloidin staining and Western blot analysis demonstrated that Src can depolymerize the actin cytoskeleton and dephosphorylate Cofilin (Fig. 2). We further examined the involvement of the MEK/Erk pathway in Src-mediated modulation of the actin cytoskeleton. Treatment of MCF-10A v-Src:ER cells with the MEK inhibitor U0126 completely inhibited Src-mediated phosphorylation of Erk1/2, a major target of MEK1/2 (Fig. 3A). Under this condition, U0126 significantly inhibited both Src-induced actin dynamics (Fig. 3B) and the dephosphorylation of Cofilin (Fig. 3C). Therefore, these results indicate that Src induces Cofilin-mediated actin depolymerization through the MEK/Erk pathway in MCF-10A cells.

We also investigated whether the MEK/Erk pathway is involved in Src-reduced *FAT4* mRNA expression by RT-qPCR analysis; the results suggest that Src-mediated inhibition of *FAT4* mRNA expression is repressed in MCF-10A cells by U0126 or PD0325901, a MEK inhibitor (Fig. 3D and S2 Fig.). In addition, to emphasize the importance of the MEK/Erk pathway in *FAT4* mRNA repression we evaluated the effect of U0126 on *FAT4* mRNA expression in MDA-MB-231 cells, a malignant breast cancer cell line. Treatment of MDA-MB-231 cells with U0126 also up-regulated *FAT4* mRNA expression (Fig. 3E). Thus, these results indicate that Src represses *FAT4* mRNA expression through the MEK/Erk pathway. Intriguingly, siRNA-
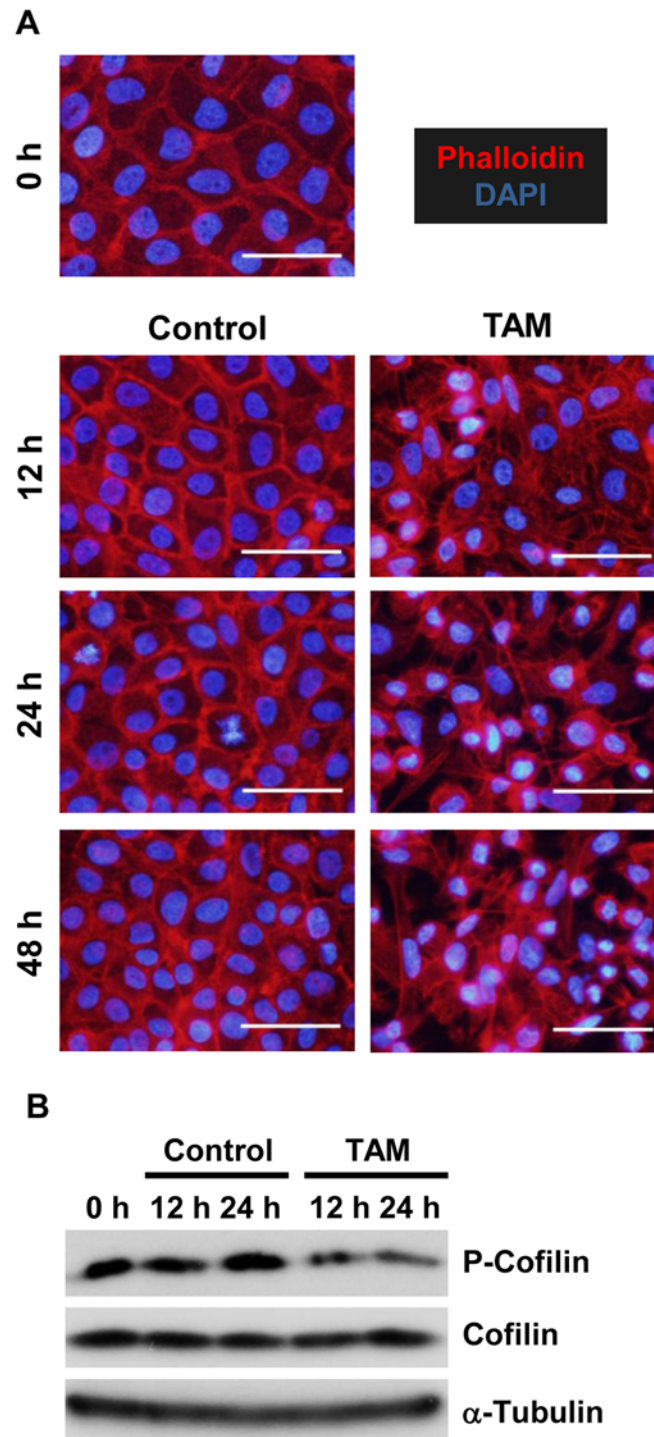
Fig 2. Src depolymerizes actin filaments via dephosphorylation of Cofilin. A. Staining for actin filaments (F-actin) (Phalloidin) and nuclei (DAPI) in TAM-treated MCF-10A v-Src:ER cells. The cells were treated with 1 µM TAM for the indicated time periods. White bars, 50 µm. **B**. Western blotting for phosphorylated and total Cofilin (P-Cofilin and Cofilin, respectively) in TAM-treated cells for the indicated time periods. Western blotting for α-Tubulin was used as a loading control.

doi:10.1371/journal.pone.0118336.g002
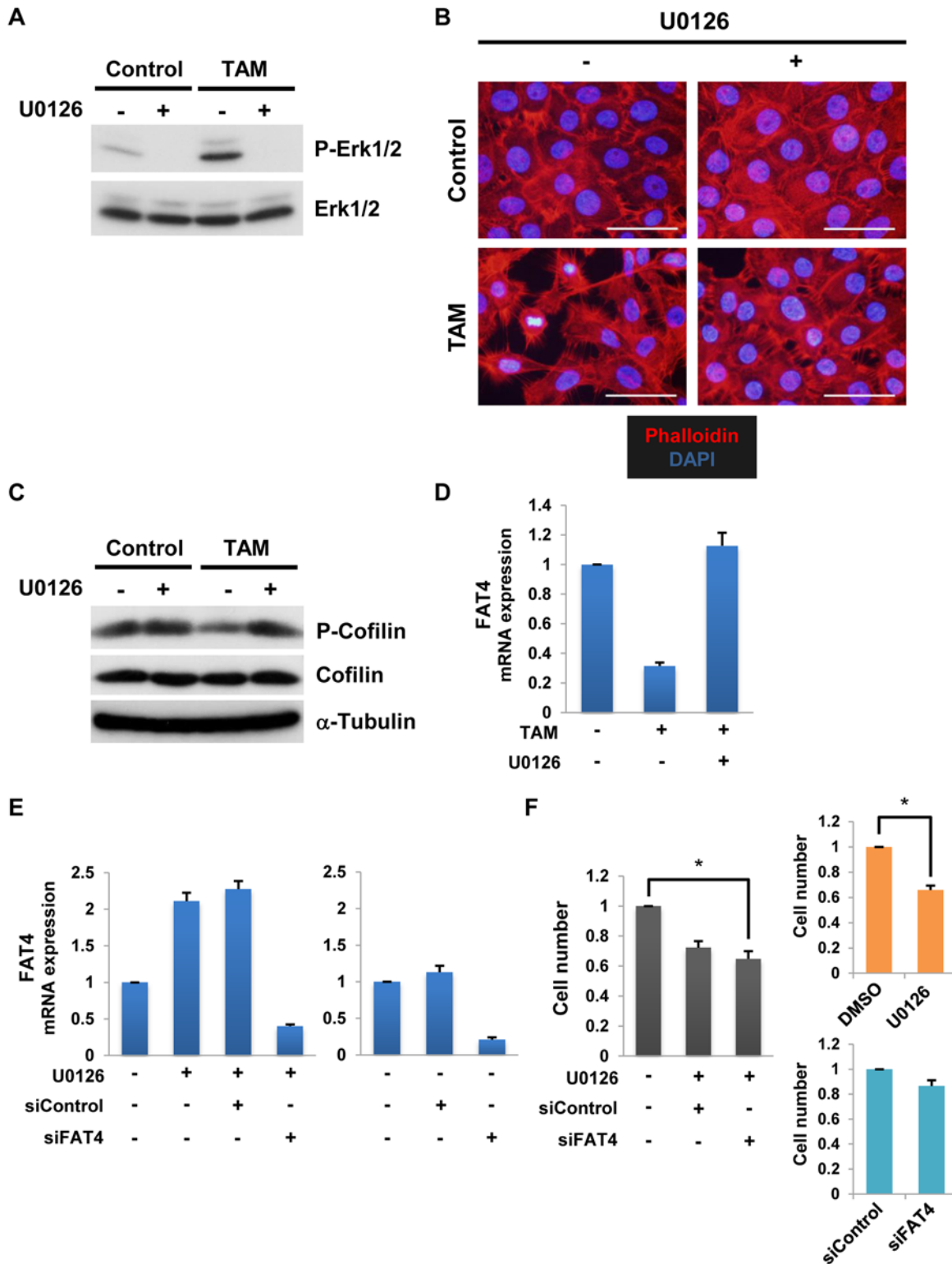
Fig 3. The MEK/Erk pathway is indispensable for both *FAT4* gene repression and Cofilin-mediated actin depolymerization by Src. A. Western blotting for phosphorylated and total Erk1/2 (P-Erk1/2 and Erk1/2, respectively) in MCF-10A v-Src:ER cells. Serum-starved cells (16 h) were cultured in the presence or absence of the MEK inhibitor U0126 for 1 h (30 µM) and then treated with 1 µM TAM for 1 h. B. Staining for F-actin (Phalloidin) and nuclei (DAPI) in TAM-treated cells (24 h) after pretreatment with 30 µM U0126 for 1 h. White bars, 50 µm. C. Western blotting for the indicated proteins in TAM-treated cells after pretreatment with U0126. D. RT-qPCR analyses of *FAT4* mRNA expression levels in TAM-treated cells after pretreatment with U0126 (mean ± SD,

n = 3). **E**. RT-qPCR analyses of *FAT4* mRNA expression levels in MDA-MB-231 cells treated with 20 μM U0126 for 24 h after pretreatment with control or FAT4 siRNA (siControl and siFAT4, respectively, 20 nM) (mean ± SD, n = 3). **F**. WST-1 Assay in U0126-treated MDA-MB-231 cells (48 h) after pretreatment with siFAT4 for 24 h (mean ± SD, n = 5, * indicates $P < 0.05$).

mediated knockdown of FAT4 did not block U0126-induced growth inhibition of MDA-MB-231 cells ([Fig. 3F](#)), perhaps because the MEK/Erk pathway regulates various targets that include *FAT4* gene. Collectively, these results suggest that Src activation induces not only Cofilin-mediated actin depolymerization but also *FAT4* mRNA repression through the MEK/Erk pathway.

Src represses *FAT4* gene expression through Cofilin1-mediated actin depolymerization

Next, we examined the causal relationship between *FAT4* mRNA repression and Cofilin-mediated actin depolymerization, both of which are downstream of the Src/MEK/Erk pathway. The ROCK pathway is a major pathway that regulates Cofilin-mediated actin depolymerization [33,34]. Thus, to determine whether Src downregulates *FAT4* mRNA expression by altering actin structures, we examined the effect of the ROCK inhibitor Y-27632 on *FAT4* mRNA expression. Treatment of MCF-10A cells with Y-27632 reduced *FAT4* mRNA expression in a dose-dependent manner ([Fig. 4A](#)). The inhibitory effect of Y-27632 on *FAT4* mRNA expression was abrogated by siRNA-mediated knockdown of Cofilin1 ([Fig. 4B](#)). Cofilin1 is a non-muscle type of Cofilin [32]. Effective knockdown of Cofilin1 was supported by RT-qPCR ([Fig. 4B](#)) and Western blot analysis ([Fig. 4C](#)). Moreover, simultaneous administration of the actin depolymerizing agent Latrunculin A, Y-27632, and siCofilin1 to the cells resulted in a striking decrease of *FAT4* mRNA expression equal to that of the Y-27632 treatment alone ([Fig. 4B](#) and [S3 Fig](#).). Phalloidin staining showed that Latrunculin A sufficiently depolymerizes the actin cytoskeleton ([Fig. 4D](#)). Therefore, on one hand, these results suggest that ROCK1/2 regulates *FAT4* mRNA expression via Cofilin1-mediated actin depolymerization. On the other hand, they suggest that inhibition of Cofilin1 significantly attenuates *FAT4* mRNA repression by Src ([Fig. 4E](#)). Therefore, we propose that Src suppresses *FAT4* mRNA expression through actin depolymerization by Cofilin1.

Mechanotransduction affects *FAT4* gene expression

Recent studies have reported that mechanical stress on cells affects cellular behavior via the modulation of actin dynamics [35–37]. Based on our findings that *FAT4* mRNA expression is regulated by actin depolmerization through Cofilin1 ([Fig. 4](#)), we examined whether mechanical stress also affects *FAT4* mRNA expression. To test this hypothesis, we performed a Cell Density Assay and a Softwell Assay. In the Cell Density Assay, MCF-10A cells were seeded at high and low cell densities to evaluate the effect of cell-cell contact on *FAT4* mRNA expression. The Softwell Assay used collagen type I-coated Softwell plates of varying degrees of stiffness (50 kPa and 0.5 kPa) to assess the effect of anchorage stiffness on *FAT4* mRNA expression. *FAT4* mRNA expression was reduced under both low cell density ([Fig. 5A](#)) and low anchorage stiffness conditions ([Fig. 5B](#)). These findings suggest that the mechanical stress that stems from the extracellular environment is intimately linked with *FAT4* mRNA expression. Moreover, we found no significant difference in phoshorylated-Cofilin expression between high and low density cells ([S4 Fig](#).). Thus, it may be assumed that the observed alteration in *FAT4* mRNA expression under low density conditions is not mediated through the MEK/ERK/Cofilin cascade.
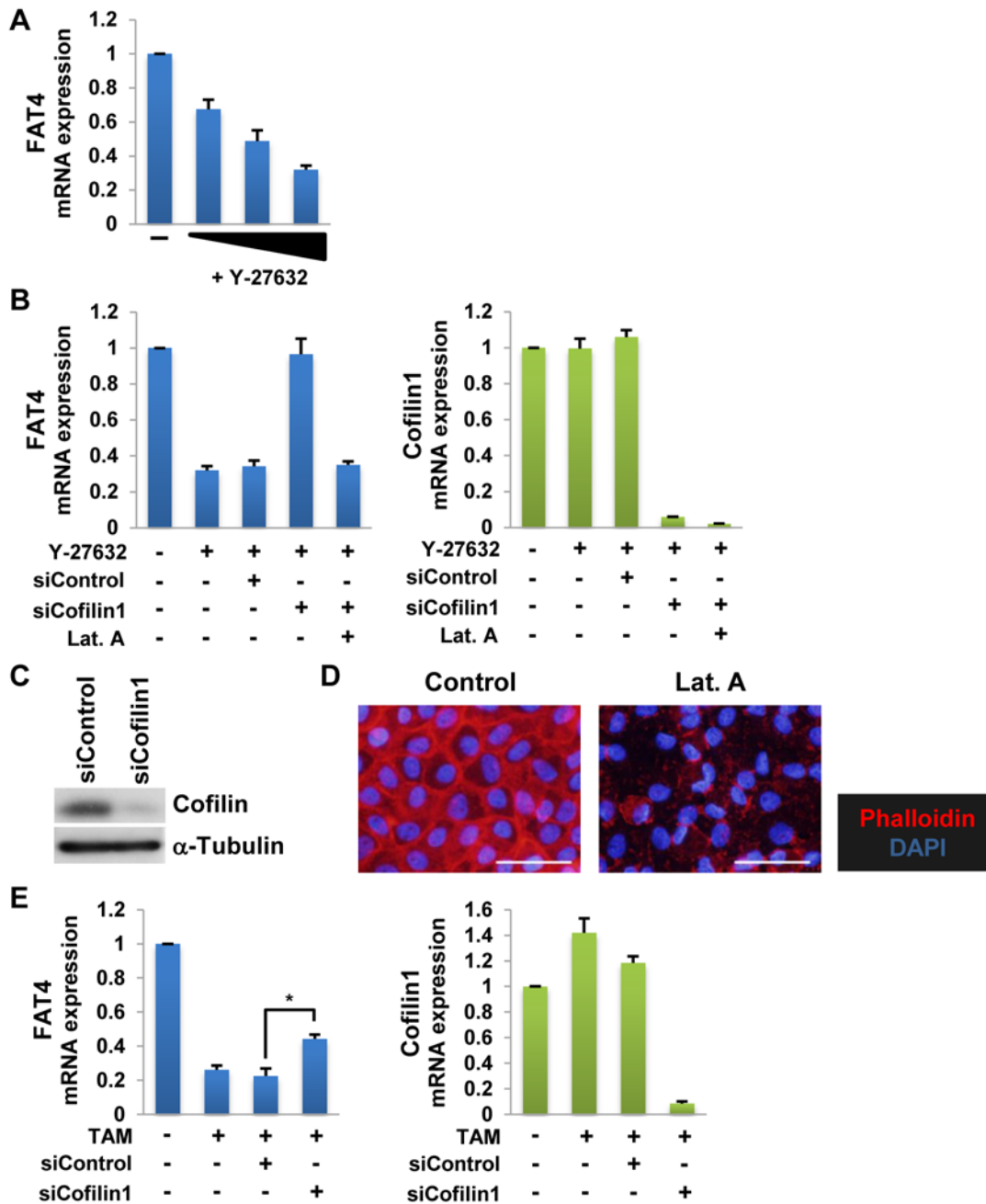
Fig 4. Src represses *FAT4* gene expression through Cofilin1-mediated actin depolymerization. A. RT-qPCR analyses of *FAT4* mRNA expression levels in MCF-10A cells treated with the ROCK inhibitor Y-27632 (10, 30 and 50 μM) for 24 h (mean ± SD, n = 3). **B**. RT-qPCR analyses of *FAT4* and *Cofilin1* mRNA expression levels in MCF-10A cells treated with 50 μM Y-27632 and 0.5 μM Latrunculin A (Lat. A) for 24 h after pretreatment with control or Cofilin1 siRNA (siControl and siCofilin1, respectively, 20 nM) (mean ± SD, n = 3). **C**. Western blotting for the indicated proteins in cells transfected with siCofilin1 for 24 h. **D**. Staining for F-actin (Phalloidin) and nuclei (DAPI) in Lat. A-treated cells (24 h). White bars, 50 μm. **E**. RT-qPCR analyses of *FAT4* and *Cofilin1* mRNA expression levels in TAM-treated MCF-10A v-Src:ER cells (24 h) after pretreatment with siCofilin1 (70 nM) (mean ± SD, n = 3, * indicates $P < 0.05$).

doi:10.1371/journal.pone.0118336.g004

FAT4 suppresses the activity of the Hippo effector YAP/TAZ

Accumulating evidence suggests that the FAT4-Hippo axis is also conserved in humans [12–14,25,26]. We next examined the effects of FAT4 knockdown on the function of the Hippo
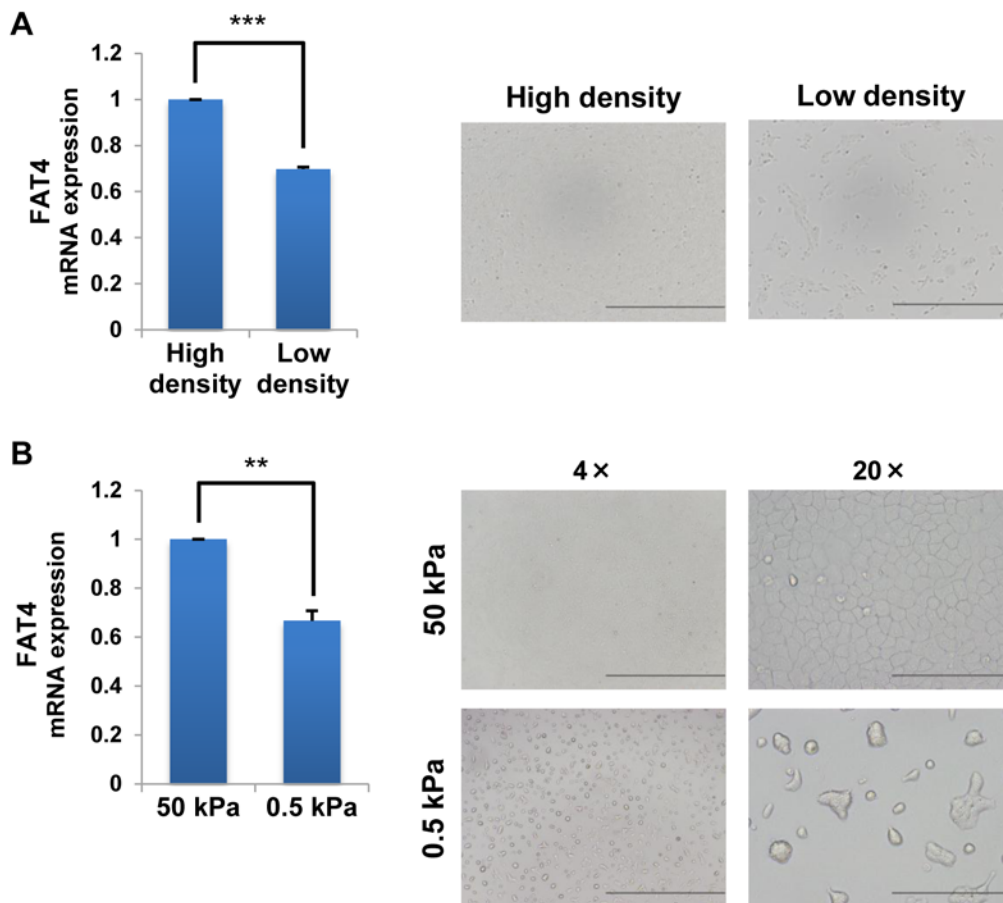
Fig 5. Mechanotransduction affects *FAT4* gene expression. A. Cell Density Assay. RT-qPCR analyses of *FAT4* and *CTGF* mRNA expression in MCF-10A cells grown under high or low cell density conditions for 24 h (4.2×10^5 cells and 7.0×10^4 cells per well on a 6-well plate, respectively) (mean ± SD, n = 3, *** indicates $P < 0.001$). Images show cells grown under high or low cell density conditions for 24 h. Black bars, 1 mm. **B**. Softwell Assay. RT-qPCR analyses of *FAT4* and *CTGF* mRNA expression in MCF-10A cells grown on stiff (50 kPa) or soft (0.5 kPa) 10 μg/ml Collagen I-coated Softwell plates for 48 h (mean ± SD, n = 3, ** indicates $P < 0.01$). Images show cells grown on the indicated stiffness for 24 h. Black bars, 1 mm or 200 μm.

doi:10.1371/journal.pone.0118336.g005

effector YAP/TAZ. YAP/TAZ activity is suppressed by cytoplasmic retention and proteasomal degradation due to LATS1/2-mediated phosphorylation of YAP/TAZ [38–42]. FAT4 siRNA increased mRNA expression levels of *CTGF*, a YAP/TAZ target gene (Fig. 6A) [18–21,23,24], by promoting the nuclear accumulation of YAP/TAZ (Fig. 6B). Furthermore, we found that the oncoprotein Src promoted YAP/TAZ activity in MCF-10A cells (Figs. 6C and 6D). These results are consistent with those of a recent study that demonstrated *Drosophila* Src64B activates Yorkie, the mammalian Yap/Taz homologue, by repressing the core components of the Hippo pathway (Hippo/Warts) [43]. Thus, our results suggest that FAT4 represses *CTGF* mRNA expression through the inactivation of YAP/TAZ.

We next examined the molecular basis of YAP/TAZ activation by FAT4 knockdown. Because YAP/TAZ activity is regulated by mechanotransduction via actin dynamics [35,36,38], we investigated the effects of FAT4 siRNA on actin dynamics. Phalloidin staining revealed that FAT4 knockdown induced abnormal spiny actin structures that radiated in all directions from the cells (Fig. 6E and S5 Fig.). However, this structural modulation of actin was independent of Cofilin because we observed no increase in phosphorylated Cofilin (Fig. 6F). Taken together, our results may suggest that FAT4 represses YAP/TAZ activity by regulating actin structures.
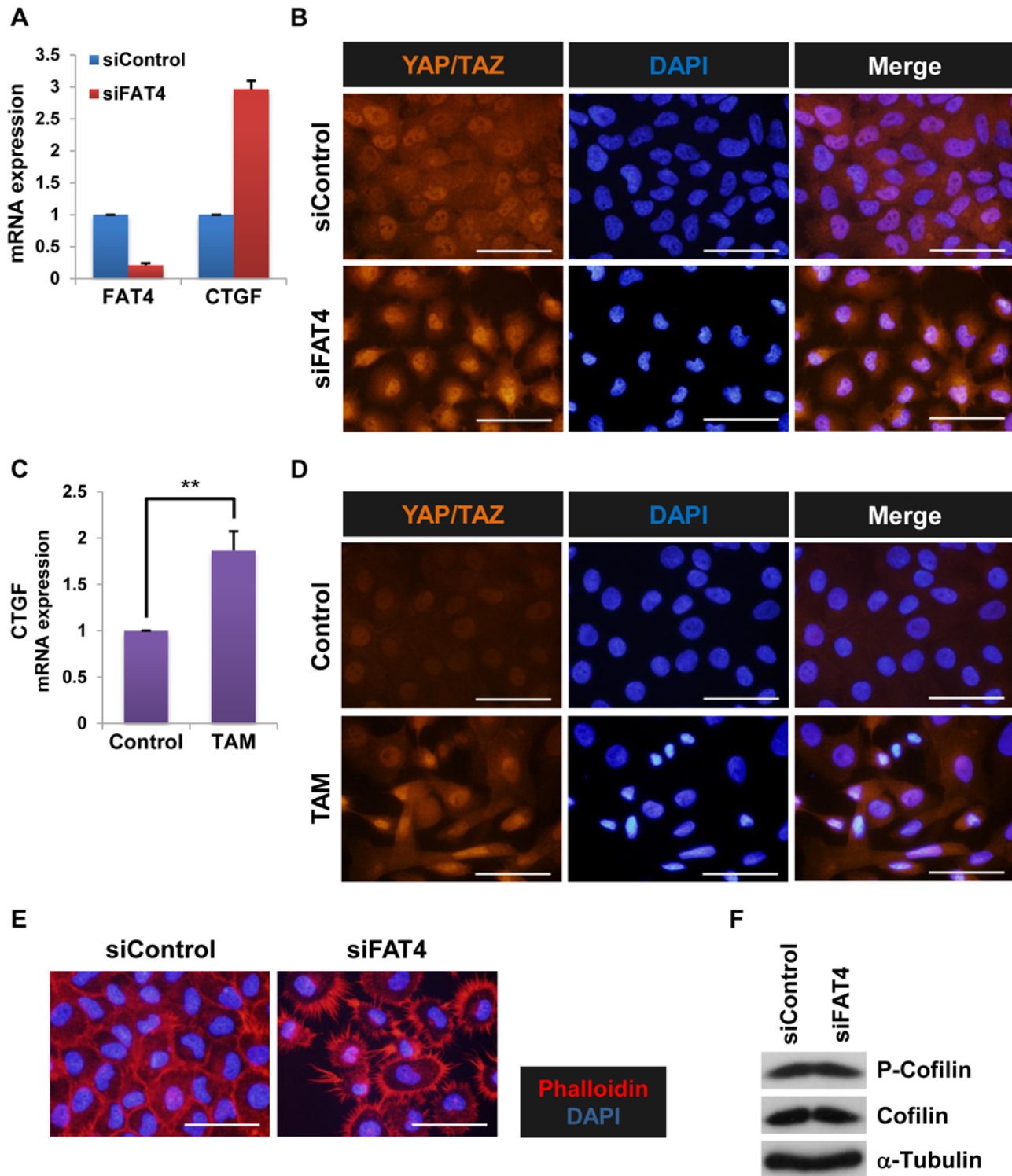
Fig 6. FAT4 negatively regulates the activity of the Hippo effector YAP/TAZ. A. RT-qPCR analyses of *FAT4* and *CTGF* mRNA levels in MCF-10A cells transfected with control or FAT4 siRNA (siControl and siFAT4, respectively, 30 nM) for 48 h (mean ± SD, n = 3). **B**. Immunofluorescence images of YAP/TAZ in MCF-10A cells transfected with siFAT4 for 48 h. The nuclei were stained with DAPI. White bars, 50 μm. **C**. RT-qPCR analysis of *CTGF* mRNA expression levels in 24 h TAM-treated MCF-10A v-Src:ER cells (mean ± SD, n = 3, ** indicates $P < 0.01$). **D**. Immunofluorescence images of YAP/TAZ in TAM-treated cells (24 h). The nuclei were stained with DAPI. White bars, 50 μm. **E**. Staining for F-actin (Phalloidin) and nuclei (DAPI) in cells transfected with siFAT4 for 48 h. White bars, 50 μm. **F**. Western blotting for the indicated proteins in 48 h siFAT4-treated cells.

doi:10.1371/journal.pone.0118336.g006

FAT4 knockdown does not induce cell transformation

Finally, we investigated whether FAT4 knockdown alone can transform MCF-10A cells because FAT4 knockdown activates YAP/TAZ, which elicits cell transformation (Figs. 6A and 6B) [23,24]. However, FAT4 knockdown alone did not cause increased cell proliferation nor anchorage-independent growth in MCF-10A cells (S6 Fig.). Therefore, combinatorial effects of reduced *FAT4* gene expression and other factors could be necessary for tumor transformation in MCF-10A cells.

Discussion

Reduced *FAT4* gene expression in human breast cancers has been reported in several studies [11,12]. Nevertheless, the molecular mechanism that governs this down-regulation in gene expression remains unknown. Here, we show that *FAT4* mRNA expression is repressed in response to actin dynamics during Src-induced tumor transformation of MCF-10A cells (Fig. 7). Src-mediated actin depolymerization is regulated by the MEK/Erk/Cofilin1 cascade and results in the repression of *FAT4* mRNA expression. Finally, we demonstrate that reduced expression of FAT4 induces the activity of the Hippo effector YAP/TAZ in MCF-10A cells. Altogether, these results propose a novel mechanism by which actin dynamics regulate cancer-related traits through the loss of FAT4-mediated cell-cell adhesion.
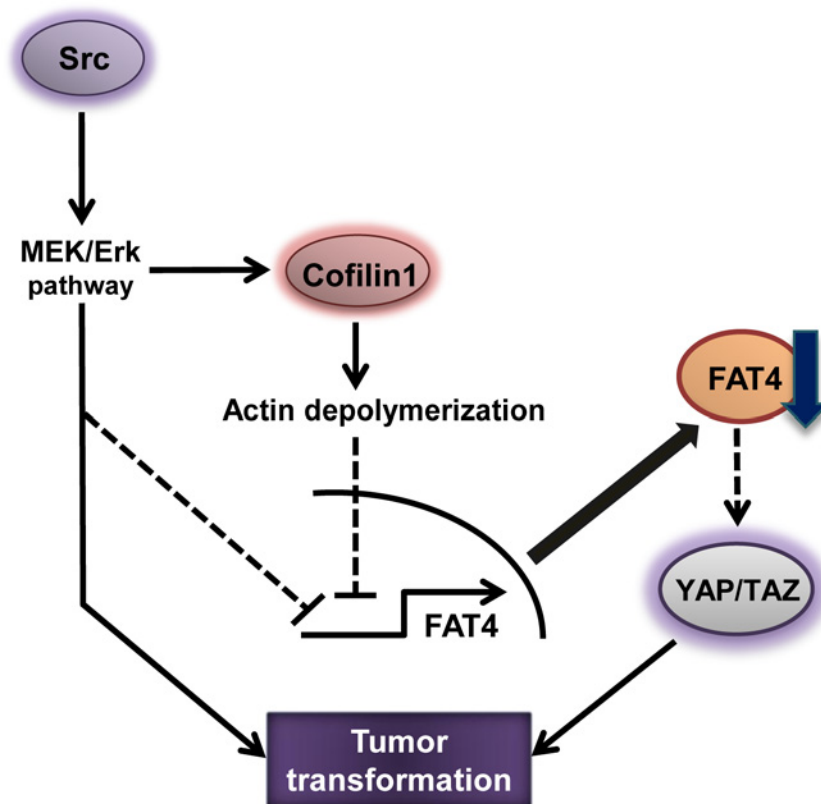

Fig 7. A model of *FAT4* gene repression in Src-induced tumorigenesis. Src activation represses *FAT4* gene expression through the MEK/Erk/Cofilin1 cascade, which induces actin depolymerization in tumor transformation. *FAT4* gene repression further elicits YAP/TAZ activation.

doi:10.1371/journal.pone.0118336.g007

In this study, we demonstrate that the Src/MEK/Erk/Cofilin1 cascade, which mediates actin depolymerization, represses *FAT4* gene expression in MCF-10A cells (Fig. 7). The mechanism by which the MEK/Erk pathway represses *FAT4* gene expression is conserved in even the malignant breast cancer cell line MDA-MB-231 cells as well as the normal breast cell line MCF-10A cells (Fig. 3D and 3E). Src activates Cofilin via dephosphorylation by components of the MEK/Erk pathway (Fig. 3C) and thereby induces actin depolymerization (Fig. 3B). Notably, the MEK/Erk pathway plays an important role in activating Cofilin in a variety of human cancer cell lines [5,44–47]. Moreover, simultaneous administration of the ROCK inhibitor Y-27632 and siCofilin1 lead to restore *FAT4* mRNA expression repressed by Y-27632 in the cells (Fig. 4B). Thus, these results suggest that Src-Cofilin1 axis plays an important role in the regulation of *FAT4* mRNA expression in breast cancer cells. Unexpectedly, the siRNA-mediated Cofilin knockdown did not completely block the reduction in *FAT4* mRNA expression by Src, although it abolished the inhibitory effect of Y-27632 on *FAT4* mRNA expression (Fig. 4B and 4E). Generally, Src regulates a wider array of signaling pathways than ROCK. As such, this may result in the significant differences presented in these data. Taken together, these results clearly show the inhibitory effect of Src on *FAT4* mRNA expression in response to actin dynamics during carcinogenesis.

The molecular mechanisms by which Src-induced actin depolymerization represses *FAT4* mRNA expression have not yet been elucidated. The *FAT4* gene is silenced by promoter hypermethylation in breast cancer cells [12]. Interestingly, Src elicits the overexpression of DNA methyltransferase (DNMT) 1 and induces DNA hypermethylation in rat 3Y1 fibroblasts [48]. Additionally, the MEK/Erk pathway induces DNA hypermethylation via the regulation of DNMT1 [49–51]. Therefore, Src-induced actin depolymerization has been speculated to repress *FAT4* mRNA expression via DNMT1-induced promoter hypermethylation during carcinogenesis, but further studies are needed for clarification.

Our study demonstrates that siRNA-mediated knockdown of FAT4 induces YAP/TAZ activity in MCF-10A cells (Fig. 6A and 6B). In line with this view, recent studies utilizing *in vivo* electroporation have demonstrated that Fat4 downregulates Yap activity leading to the inhibition of neural progenitor cell proliferation during murine and avian neurogenesis [25,26]. In addition, it has been demonstrated that deletion of Fat4 in mice causes primarily the nuclear accumulation of Yap in the nephron progenitor cells [52]. As such, these *in vivo* findings suggest that the Fat4-Hippo axis is highly conserved in mammals. However, the molecular underpinnings of Fat4-mediated nuclear translocation of Yap/Taz in mammals still remain unknown. Because there is no mammalian counterpart of *Drosophila* Dachs, which is regulated by Fat to activate the Hippo pathway [9,10,18], Fat4 should modulate Yap/Taz activity differently from Fat. In this regard, our research demonstrates that YAP phosphorylation levels (at least at Ser127) in FAT4 siRNA-treated cells are consistent with those found in control siRNA-treated MCF-10A cells (S7 Fig.). Nevertheless, MST1 kinase (mammalian Hippo ortholog) expression is reduced in FAT4 siRNA-treated cells (S7 Fig.). Accordingly, it is possible that nuclear localization of YAP is regulated by FAT4 through a Ser127 phosphorylation-independent mechanism.

It is also known that FAT4 is involved in the maintenance of planar cell polarity (PCP) [9]. Indeed, Fat4 mutant mice and PCP gene mutant mice show similar defects of the inner ear such as significant disruptions in orientation of hair cells and elongation of the cochlea [53]. Moreover, PCP genes have also been shown to regulate actin dynamics [54]. Collectively, these findings suggest that Fat4 regulates actin dynamics as well as vertebrate PCP. Interestingly, YAP/TAZ activity can be modulated by cytoskeletal tension induced by cell spreading in a Hippo pathway-independent manner [10,21,35]. Therefore, we can surmise that FAT4 regulates the YAP/TAZ activity through modulating actin cytoskeleton. In fact, we show that FAT4

knockdown induces abnormal spiny actin protrusions, which may enhance cell spreading (Fig. 6E). Thus, FAT4 may negatively regulate YAP/TAZ function by modulating actin cyto-skeletal tension. Altogether, our current study presents a novel model in which FAT4 represses YAP/TAZ activity by regulating actin structures, at least in breast cancer cells. Further examination is needed to elucidate the molecular basis of YAP/TAZ inactivation by FAT4.

Accumulating evidences suggest the pathophysiological relevance between FAT4 reduction and carcinogenesis. Qi et al. have clearly demonstrated that *FAT4* mRNA is not expressed at all in many breast cancer cell lines (BT20, ZR75–1, and BT474 cells) [12]. We also found that MCF-7 breast cancer cells express far too low a level of *FAT4* mRNA compared with the MCF-10A normal mammary cell line (data not shown). Moreover, FAT4 knockdown has been shown to induce the malignant phenotype of human gastric cancer cell lines [55]. However, we show that FAT4 knockdown alone is not sufficient to induce cell proliferation or anchorage-independent growth in MCF-10A cells despite promoting YAP/TAZ activity (S6 Fig.; Fig. 6A and 6B); nevertheless, overexpression of YAP/TAZ can transform the cells [23,24]. Additionally, FAT4 knock-down alone does not induce cell proliferation in malignant breast cancer MDA-MB-231 cells (Fig. 3F). These data strongly demonstrate that cooperative effects between FAT4 reduction and other factors induce tumor transformation in MCF-10A cells. We propose that the MEK/Erk pathway involves in the Src-induced tumorigenesis as well as *FAT4* mRNA repression (Fig. 3A-D), because numerous studies have already established the importance of the MEK/Erk pathway for cell transformation [2,5,44,56,57]. Further comprehensive analyses are required to solve molecular mechanisms of Src-mediated carcinogenesis through repressing *FAT4* gene expression.

Materials and Methods

Cell culture and generation of stable cell lines

MCF-10A cells are immortalized normal human mammary epithelial cells that do not express the estrogen receptor (ER) [27,29]. MCF-10A cells were obtained from the American Type Culture Collection (ATCC). We generated MCF-10A cells stably expressing v-Src:ER chimeras (MCF-10A v-Src:ER) by using retroviruses and transformed them with 1 μM 4-Hydroxyta-moxifen (H7904; Sigma) or the solvent ethanol as a control. MCF-10A cells were cultured in Assay Medium. Assay Medium is DMEM/F12 media (1:1) (11320–033; Gibco) supplemented with 2% horse serum (16050–122; Gibco), 0.5 μg/ml hydrocortisone (H4001; Sigma), 10 μg/ml insulin (093–06351; Wako), 100 ng/ml Cholera toxin (C8052; Sigma) and penicillin-strepto-mycin (15140–122; Gibco). In both siRNA knockdown experiments and Soft Agar Colony Formation Assays, Growth Medium was used as culture medium. Growth Medium is DMEM/F12 media (1:1) supplemented with 5% horse serum, 0.5 μg/ml hydrocortisone, 10 μg/ml insulin, 20 ng/ml epidermal growth factor (AF-100–15; PeproTech), 100 ng/ml Cholera toxin and penicillin-streptomycin. MDA-MB-231 cells, which are malignant mammary cancer cells, were cultured in DMEM/F12 media (1:1) supplemented with 10% FBS and penicillin-streptomycin. All cell lines were incubated at 37°C in a humidified atmosphere containing 5% CO_2.

Chemicals

The chemicals used in this study included U0126 (662005; Calbiochem), Y-27632 (257–00511; Wako), and Latrunculin A (sc-202691; Santa Cruz).

Antibodies

The antibodies in this study included anti-α-tubulin (DM1A; Sigma), anti-Erk1/2 (137F5; Cell Signaling Technology), anti-Phospho-Erk1/2 (D13.14.4E; Cell Signaling Technology), anti-

Cofilin (ACFL02; Cytoskeleton), anti-Phospho-Cofilin (Ser3) (#3311; Cell Signaling Technology), and anti-YAP (sc101199; Santa Cruz) (detects both YAP and TAZ).

siRNA knockdown experiments

Cells were cultured in Growth Medium without antibiotics at 37°C for 24 h and were then transfected with siRNA using both Lipofectamine RNAiMAX (Invitrogen) and Opti-MEM I Reduced Serum Medium (31985–070; Gibco) according to the manufacturer's protocol. The sequences of the siRNAs employed in this study are listed in S1 Table. The siRNA concentrations are described in the Figure Legends.

RNA extraction and real-time quantitative PCR (RT-qPCR)

Total RNA was extracted from cells with ISOGENII (311–07361; Wako) or the RNeasy Mini Kit (Qiagen) and was subjected to cDNA synthesis with random hexamer primers and Moloney murine leukemia virus (M-MLV) reverse transcriptase (Invitrogen) according to the manufacturer's protocols. RT-qPCR was performed with FastStart Universal SYBR (Roche) and a Thermal Cycler Dice Real Time System II (TP900; Takara Bio). The PCR primers that were used are listed in S2 Table. 18S rRNA was used for normalization.

Western blotting

The cells were lysed in buffer containing 1% Triton X-100, 1% sodium deoxycholate, 0.1% SDS, 20 mM Tris-HCl, pH 7.5, 150 mM NaCl, 10 mM EDTA, 1 mM EGTA, 10% glycerol, 2.5 mM sodium pyrophosphate, 1 mM β-glycerophosphate, 1 mM sodium vanadate, and 1x protease inhibitor cocktail (Roche). Cellular debris was removed by centrifuging at 10 minutes at 13,000 xg at 4°C. Protein concentrations were determined with a Pierce BCA Protein Assay kit. Protein samples were loaded on 7%–12% SDS-polyacrylamide gels, separated, and transferred to Immobilon-P Membranes (IPVH00010; Merck). Membranes were blocked with Blocking One (03953–95; Nacalai tesque) and incubated with the antibodies indicated in the figures. The blots were treated with a horseradish peroxidase-conjugated secondary antibody (Invitrogen) and were developed with an enhanced chemiluminescence (ECL) kit (RPN2106; GE Healthcare). All original uncropped and unadjusted blots are shown in S8 Fig.

Fluorescent staining

The cells were fixed with 4% formaldehyde solution in PBS on ice for 15 min, washed 3 times, and were permeabilized with 0.5% Triton X-100 in PBS for 10 min at room temperature (RT). After blocking cells with PBS containing 1% skim milk for 20 min at RT, the cells were incubated overnight at 4°C with anti-YAP antibody diluted in PBS containing 1% skim milk. After washing the cells 3 times with PBS, the cells were incubated with Alexa Fluor 546-conjugated secondary antibody (A-11030; Invitrogen) diluted in PBS containing 1% skim milk for 1 h at RT. To stain actin filaments (F-actin), the cells were blocked with PBS containing 5% BSA for 30 min at RT and were incubated with CF594 Phalloidin (00045; Biotium) in PBS containing 1% BSA for 20 min at RT, followed by PBS washes. The nuclei were stained with 4',6'-diamidino-2-phenylindole (DAPI) (100 ng/ml) for 10 min at RT. Finally, the cells were sealed with fluorescence mounting medium (S3023; Dako). Fluorescent images were captured with an Olympus LX71 fluorescence microscope.

WST-1 Assay

The cells were seeded at 4.0×10^3 cells per well (96-well plate), cultured for 16 h and treated with TAM at 37°C for 48 h. For siRNA-mediated FAT4 knockdown experiments, MCF-10A cells were treated with FAT4 siRNA by reverse transfection according to the manufacturer's protocol. The cells were seeded at 2.8×10^3 cells per well (96-well plate) and incubated at 37°C for 48 h. On the other hand, MDA-MB-231 cells were seeded at 3.7×10^3 cells per well (96-well plate), cultured for 24 h and treated with U0126 at 37°C for 48 h. For siRNA-mediated FAT4 knockdown experiments by reverse transfection, the cells were seeded at 2.5×10^3 cells per well (96-well plate) and incubated at 37°C for 72 h or otherwise 24 h followed by treatment with U0126 for 48 h. Next, WST-1 reagent (5015944; Roche) was added to the cells for a 2 h incubation at 37°C. After shaking for 1 min, the viability of the cells was analyzed by a Microplate Reader (Molecular Devices) at 450 nm with a reference wavelength of 650 nm.

Soft Agar Colony Formation Assay

The cells were seeded at 4.6×10^5 cells (6 cm dish), cultured in Assay Medium at 37°C for 24 h and were then treated with TAM at 37°C for 72 h before the colony formation assay. For siRNA-mediated FAT4 knockdown experiments, the cells were seeded at 1.8×10^5 cells (6 cm dish) and cultured in Growth Medium without antibiotics at 37°C for 24 h. The cells were then transfected twice with FAT4 or control siRNA (at 24 h and 48 h after plating) and cultured for a further 24 h after the last transfection. Subsequently, the cells were seeded at 7.0×10^2 cells per well (96-well plate) in Growth Medium containing 0.4% agarose (100 µl) onto a lower layer of Growth Medium containing 0.5% agar (100 µl). Cells were fed 2 times per a week. The number of colonies was counted after 14 days.

Cell Density Assay

The cells were seeded at 4.2×10^5 cells (High density) or 7.0×10^4 (Low density) cells per well (6-well plate), cultured in Assay Medium at 37°C for 24 h and subjected to RT-qPCR analysis.

Softwell Assay

Twenty-four well Softwell plates of two different qualities of stiffness (50 kPa: stiff or 0.5 kPa: soft) (Matrigen) were coated by Collagen I, rat tail (354236, BD Biosciences) (10°g/ml) for 1 h at RT. The cells were seeded at 8.1×10^4 cells per well in Softwell plates. The cells were cultured in Assay Medium for 48 h and subjected to RT-qPCR analysis.

Statistical analyses

Statistical analyses were performed using Student's t-test; a $P < 0.05$ was considered significant.

Supporting Information

S1 Fig. Transient activation of Src does not alter *TWIST1* gene expression. RT-qPCR analysis of *TWIST1* mRNA expression levels in TAM-treated MCF-10A v-Src:ER cells for the indicated times (mean ± SD, n = 3).
(TIF)

S2 Fig. PD0325901, a MEK inhibitor, blocks the inhibitory effect of Src on *FAT4* mRNA expression in MCF-10A cells. RT-qPCR analyses of *FAT4* mRNA expression levels in TAM-treated cells following pretreatment with PD0325901 (444968; Calbiochem) (mean ± SD,

n = 3).
(TIF)

S3 Fig. Cofilin siRNA inhibits Latrunculin A-mediated reduction of *FAT4* mRNA expression. RT-qPCR analyses of *FAT4* mRNA expression levels in MCF-10A cells treated with 0.5 μM Latrunculin A (Lat. A) for 24 h following pretreatment with either control or Cofilin1 siRNA (siControl and siCofilin1, respectively, 20 nM) (mean ± SD, n = 3).
(TIF)

S4 Fig. Phoshorylated-Cofilin expression is similar in high and low density MCF-10A cells. Western blotting for α-Tubulin and phosphorylated Cofilin in MCF-10A cells under high or low cell density conditions.
(TIF)

S5 Fig. The effect of FAT4 knockdown on actin protrusions in low density MCF-10A cells. Staining for F-actin (Phalloidin) and nuclei (DAPI) in cells transfected with siControl or siFAT4 for 48 h. Abnormal spiny actin protrusions are indicated by white arrowheads. White bars, 50 μm.
(TIF)

S6 Fig. The effects of FAT4 knockdown on cell proliferation and anchorage-independent growth. A. WST-1 Assay in MCF-10A cells after treatment with FAT4 siRNA for 48 h (siFAT4, 30 nM) (mean ± SD, n = 4). **B**. Soft Agar Colony Formation Assay in MCF-10A cells after treatment with siFAT4 for 72 h (30 nM) (mean ± SD, n = 6). Images show the cell colonies. Black bars, 1 mm.
(TIF)

S7 Fig. FAT4 knockdown in MCF-10A cells does not alter phosphorylated YAP expression but reduces MST1 expression. Western blotting for phosphorylated YAP (Ser127) (#4911; Cell Signaling Technology), MST1 (#3682; Cell Signaling Technology), and α-Tubulin in MCF-10A cells. The cells were treated with control or FAT4 siRNA (siControl and siFAT4).
(TIF)

S8 Fig. Original uncropped and unadjusted blots with molecular size markers.
(TIF)

S1 Table. Sequences of siRNAs.
(TIF)

S2 Table. Sequences of primers used for RT-qPCR.
(TIF)

Acknowledgments

Author Contributions

Conceived and designed the experiments: TI HT KF SO AK. Performed the experiments: TI HT KF SO. Analyzed the data: TI HT KF SO. Wrote the paper: TI HT AK.

References

1. Frame MC, Fincham VJ, Carragher NO, Wyke JA. v-Src's hold over actin and cell adhesions. Nat Rev Mol Cell Biol. 2002; 3: 233–245. PMID: 11994743

2. Frame MC. Newest findings on the oldest oncogene; how activated src does it. J Cell Sci. 2004; 117: 989–998. PMID: 14996930

3. Frame MC. Src in cancer: deregulation and consequences for cell behaviour. Biochim Biophys Acta. 2002; 1602: 114–130. PMID: 12020799

4. Huveneers S, Danen EH. Adhesion signaling—crosstalk between integrins, Src and Rho. J Cell Sci. 2009; 122: 1059–1069. doi: 10.1242/jcs.039446 PMID: 19339545

5. Pawlak G, Helfman DM. MEK mediates v-Src-induced disruption of the actin cytoskeleton via inactivation of the Rho-ROCK-LIM kinase pathway. J Biol Chem. 2002; 277: 26927–26933. PMID: 12011049

6. Kalluri R, Weinberg RA. The basics of epithelial-mesenchymal transition. J Clin Invest. 2009; 119: 1420–1428. doi: 10.1172/JCl39104 PMID: 19487818

7. Nagathihalli NS, Merchant NB. Src-mediated regulation of E-cadherin and EMT in pancreatic cancer. Front Biosci (Landmark Ed). 2012; 17: 2059–2069. PMID: 22652764

8. Nam JS, Ino Y, Sakamoto M, Hirohashi S. Src family kinase inhibitor PP2 restores the E-cadherin/catenin cell adhesion system in human cancer cells and reduces cancer metastasis. Clin Cancer Res. 2002; 8: 2430–2436. PMID: 12114449

9. Katoh M. Function and cancer genomics of FAT family genes (review). Int J Oncol. 2012; 41: 1913–1918. doi: 10.3892/ijo.2012.1669 PMID: 23076869

10. Reddy BV, Irvine KD. The Fat and Warts signaling pathways: new insights into their regulation, mechanism and conservation. Development. 2008; 135: 2827–2838. doi: 10.1242/dev.020974 PMID: 18697904

11. Mizuno H, Kitada K, Nakai K, Sarai A. PrognoScan: a new database for meta-analysis of the prognostic value of genes. BMC Med Genomics. 2009; 2: 18. doi: 10.1186/1755-8794-2-18 PMID: 19393097

12. Qi C, Zhu YT, Hu L, Zhu YJ. Identification of Fat4 as a candidate tumor suppressor gene in breast cancers. Int J Cancer. 2009; 124: 793–798. doi: 10.1002/ijc.23775 PMID: 19048595

13. Nikolaev SI, Rimoldi D, Iseli C, Valsesia A, Robyr D, Gehrig C, et al. Exome sequencing identifies recurrent somatic MAP2K1 and MAP2K2 mutations in melanoma. Nat Genet. 2012; 44: 133–139. doi: 10.1038/ng.1026 PMID: 22197931

14. Rauch TA, Wang Z, Wu X, Kernstine KH, Riggs AD, Pfeifer GP. DNA methylation biomarkers for lung cancer. Tumour Biol. 2012; 33: 287–296. doi: 10.1007/s13277-011-0282-2 PMID: 22143938

15. Grusche FA, Richardson HE, Harvey KF. Upstream regulation of the hippo size control pathway. Curr Biol. 2010; 20: R574–R582. doi: 10.1016/j.cub.2010.05.023 PMID: 20619814

16. Staley BK, Irvine KD. Hippo signaling in Drosophila: recent advances and insights. Dev Dyn. 2012; 241: 3–15. doi: 10.1002/dvdy.22723 PMID: 22174083

17. Yu FX, Guan KL. The Hippo pathway: regulators and regulations. Genes Dev. 2013; 27: 355–371. doi: 10.1101/gad.210773.112 PMID: 23431053

18. Pan D. The hippo signaling pathway in development and cancer. Dev Cell. 2010; 19: 491–505. doi: 10.1016/j.devcel.2010.09.011 PMID: 20951342

19. Ramos A, Camargo FD. The Hippo signaling pathway and stem cell biology. Trends Cell Biol. 2012; 22: 339–346. doi: 10.1016/j.tcb.2012.04.006 PMID: 22658639

20. Zhao B, Li L, Lei Q, Guan KL. The Hippo-YAP pathway in organ size control and tumorigenesis: an updated version. Genes Dev. 2010; 24: 862–874. doi: 10.1101/gad.1909210 PMID: 20439427

21. Badouel C, McNeill H. SnapShot: The hippo signaling pathway. Cell. 2011; 145: 484–484. doi: 10.1016/j.cell.2011.04.009 PMID: 21529719

22. Sudol M, Harvey KF. Modularity in the Hippo signaling pathway. Trends Biochem Sci. 2010; 35: 627–633. doi: 10.1016/j.tibs.2010.05.010 PMID: 20598891

23. Zhang H, Liu CY, Zha ZY, Zhao B, Yao J, Zhao S, et al. TEAD transcription factors mediate the function of TAZ in cell growth and epithelial-mesenchymal transition. J Biol Chem. 2009; 284: 13355–13362. doi: 10.1074/jbc.M900843200 PMID: 19324877

24. Zhao B, Ye X, Yu J, Li L, Li W, Li S, et al. TEAD mediates YAP-dependent gene induction and growth control. Genes Dev. 2008; 22: 1962–1971. doi: 10.1101/gad.1664408 PMID: 18579750

25. Cappello S, Gray MJ, Badouel C, Lange S, Einsiedler M, Srour M, et al. Mutations in genes encoding the cadherin receptor-ligand pair DCHS1 and FAT4 disrupt cerebral cortical development. Nat Genet. 2013; 45: 1300–1308. doi: 10.1038/ng.2765 PMID: 24056717

26. Van Hateren NJ, Das RM, Hautbergue GM, Borycki AG, Placzek M, Wilson SA. FatJ acts via the Hippo mediator Yap1 to restrict the size of neural progenitor cell pools. Development. 2011; 138: 1893–1902. doi: 10.1242/dev.064204 PMID: 21521736

27. Debnath J, Muthuswamy SK, Brugge JS. Morphogenesis and oncogenesis of MCF-10A mammary epithelial acini grown in three-dimensional basement membrane cultures. Methods. 2003; 30: 256–268. PMID: 12798140

28. Hirsch HA, Iliopoulos D, Tsichlis PN, Struhl K. Metformin selectively targets cancer stem cells, and acts together with chemotherapy to block tumor growth and prolong remission. Cancer Res. 2009; 69: 7507–7511. doi: 10.1158/0008-5472.CAN-09-2994 PMID: 19752085

29. Soule HD, Maloney TM, Wolman SR, Peterson WD Jr, Brenz R, McGrath CM, et al. Isolation and characterization of a spontaneously immortalized human breast epithelial cell line, MCF-10. Cancer Res. 1990; 50: 6075–6086. PMID: 1975513

30. Iliopoulos D, Hirsch HA, Struhl K. An epigenetic switch involving NF-kappaB, Lin28, Let-7 MicroRNA, and IL6 links inflammation to cell transformation. Cell. 2009; 139: 693–706. doi: 10.1016/j.cell.2009.10.014 PMID: 19878981

31. Littlewood TD, Hancock DC, Danielian PS, Parker MG, Evan GI. A modified oestrogen receptor ligand-binding domain as an improved switch for the regulation of heterologous proteins. Nucleic Acids Res. 1995; 23: 1686–1690. PMID: 7784172

32. Mizuno K. Signaling mechanisms and functional roles of cofilin phosphorylation and dephosphorylation. Cell Signal. 2013; 25: 457–469. doi: 10.1016/j.cellsig.2012.11.001 PMID: 23153585

33. Maekawa M, Ishizaki T, Boku S, Watanabe N, Fujita A, Iwamatsu A, et al. Signaling from Rho to the actin cytoskeleton through protein kinases ROCK and LIM-kinase. Science. 1999; 285: 895–898. PMID: 10436159

34. Burridge K, Wennerberg K. Rho and Rac take center stage. Cell. 2004; 116: 167–179. PMID: 14744429

35. Dupont S, Morsut L, Aragona M, Enzo E, Giulitti S, Cordenonsi M, et al. Role of YAP/TAZ in mechano-transduction. Nature. 2011; 474: 179–183. doi: 10.1038/nature10137 PMID: 21654799

36. Aragona M, Panciera T, Manfrin A, Giulitti S, Michielin F, Elvassore N, et al. A mechanical checkpoint controls multicellular growth through YAP/TAZ regulation by actin-processing factors. Cell. 2013; 154: 1047–1059. doi: 10.1016/j.cell.2013.07.042 PMID: 23954413

37. Olson EN, Nordheim A. Linking actin dynamics and gene transcription to drive cellular motile functions. Nat Rev Mol Cell Biol. 2010; 11: 353–365. doi: 10.1038/nrm2890 PMID: 20414257

38. Zhao B, Wei X, Li W, Udan RS, Yang Q, Kim J, et al. Inactivation of YAP oncoprotein by the Hippo pathway is involved in cell contact inhibition and tissue growth control. Genes Dev. 2007; 21: 2747–2761. PMID: 17974916

39. Lei QY, Zhang H, Zhao B, Zha ZY, Bai F, Pei XH, et al. TAZ promotes cell proliferation and epithelial-mesenchymal transition and is inhibited by the hippo pathway. Mol Cell Biol. 2008; 28: 2426–2436. doi: 10.1128/MCB.01874-07 PMID: 18227151

40. Zhao B, Li L, Tumaneng K, Wang CY, Guan KL. A coordinated phosphorylation by Lats and CK1 regulates YAP stability through SCF(beta-TRCP). Genes Dev. 2010; 24: 72–85. doi: 10.1101/gad.1843810 PMID: 20048001

41. Liu CY, Zha ZY, Zhou X, Zhang H, Huang W, Zhao D, et al. The hippo tumor pathway promotes TAZ degradation by phosphorylating a phosphodegron and recruiting the SCF{beta}-TrCP E3 ligase. J Biol Chem. 2010; 285: 37159–37169. doi: 10.1074/jbc.M110.152942 PMID: 20858893

42. Liu C, Huang W, Lei Q. Regulation and function of the TAZ transcription co-activator. Int J Biochem Mol Biol. 2011; 2: 247–256. PMID: 22003437

43. Enomoto M, Igaki T. Src controls tumorigenesis via JNK-dependent regulation of the Hippo pathway in Drosophila. EMBO Rep. 2013; 14: 65–72. doi: 10.1038/embor.2012.185 PMID: 23196366

44. Pawlak G, Helfman DM. Post-transcriptional down-regulation of ROCKI/Rho-kinase through an MEK-dependent pathway leads to cytoskeleton disruption in Ras-transformed fibroblasts. Mol Biol Cell. 2002; 13: 336–347. PMID: 11809843

45. Pritchard CA, Hayes L, Wojnowski L, Zimmer A, Marais RM, Norman JC. B-Raf acts via the ROCKII/LIMK/cofilin pathway to maintain actin stress fibers in fibroblasts. Mol Cell Biol. 2004; 24: 5937–5952. PMID: 15199148

46. Lee S, Helfman DM. Cytoplasmic p21Cip1 is involved in Ras-induced inhibition of the ROCK/LIMK/cofilin pathway. J Biol Chem. 2004; 279: 1885–1891. PMID: 14559914

47. Choi C, Helfman DM. The Ras-ERK pathway modulates cytoskeleton organization, cell motility and lung metastasis signature genes in MDA-MB-231 LM2. Oncogene. 2013; 33: 3668–3676. doi: 10.1038/onc.2013.341 PMID: 23995792

48. Sung J, Turner J, McCarthy S, Enkemann S, Li CG, Yan P, et al. Oncogene regulation of tumor suppressor genes in tumorigenesis. Carcinogenesis. 2005; 26: 487–494. PMID: 15498783

49. Lu R, Wang X, Chen ZF, Sun DF, Tian XQ, Fang JY. Inhibition of the extracellular signal-regulated kinase/mitogen-activated protein kinase pathway decreases DNA methylation in colon cancer cells. J Biol Chem. 2007; 282: 12249–12259. PMID: 17307743

50. Lund P, Weisshaupt K, Mikeska T, Jammas D, Chen X, Kuban RJ, et al. Oncogenic HRAS suppresses clusterin expression through promoter hypermethylation. Oncogene. 2006; 25: 4890–4903. PMID: 16568090

51. Liu D, Hu S, Hou P, Jiang D, Condouris S, Xing M. Suppression of BRAF/MEK/MAP kinase pathway restores expression of iodide-metabolizing genes in thyroid cells expressing the V600E BRAF mutant. Clin Cancer Res. 2007; 13: 1341–1349. PMID: 17317846

52. Murphy AJ, Pierce J, de Caestecker C, Libes J, Neblett D, de Caestecker M, et al. Aberrant activation, nuclear localization, and phosphorylation of Yes-associated protein-1 in the embryonic kidney and Wilms tumor. Pediatr Blood Cancer. 2014; 61: 198–205. doi: 10.1002/pbc.24788 PMID: 24115727

53. Saburi S, Hester I, Fischer E, Pontoglio M, Eremina V, Gessler M, et al. Loss of Fat4 disrupts PCP signaling and oriented cell division and leads to cystic kidney disease. Nat Genet. 2008; 40: 1010–1015. doi: 10.1038/ng.179 PMID: 18604206

54. Olson EN, Nordheim A. Linking actin dynamics and gene transcription to drive cellular motile functions. Nat Rev Mol Cell Biol. 2010; 11: 353–365. doi: 10.1038/nrm2890 PMID: 20414257

55. Zang ZJ, Cutcutache I, Poon SL, Zhang SL, McPherson JR, Tao J, et al. Exome sequencing of gastric adenocarcinoma identifies recurrent somatic mutations in cell adhesion and chromatin remodeling genes. Nat Genet. 2012; 44: 570–574. doi: 10.1038/ng.2246 PMID: 22484628

56. Huber MA, Kraut N, Beug H. Molecular requirements for epithelial-mesenchymal transition during tumor progression. Curr Opin Cell Biol. 2005; 17: 548–558. PMID: 16098727

57. Edme N, Downward J, Thiery JP, Boyer B. Ras induces NBT-II epithelial cell scattering through the coordinate activities of Rac and MAPK pathways. J Cell Sci. 2002; 115: 2591–2601. PMID: 12045229